scientific reports

Check for updates

OPEN

Inhibitory influence of cationic Gemini surfactant on the dissolution rate of N80 carbon steel in 15% HCl solution

M. A. Deyab[1]✉ & Q. Mohsen[2]

Strong acids are commonly used in petroleum wells to remove scale layers from the surface of N80 C-steel pipe. The corrosive effects of these acids, on the other hand, pose a significant risk to C-steel pipes. For the first time, we discovered the anti-corrosion properties of cationic Gemini surfactant, 1,2-bis(dodecyldimethylammonio) ethane dibromide (DMAEB), for N80 C-steel pipe in acid washing solution (15.0% HCl). The DMAEB, in particular, can reduce the corrosion rate of N80 C-steel by approximately 97%. DMAEB molecules work as a mixed-type corrosion inhibitor, according to electrochemical results. The DMAEB demonstrated a high inhibition effect at high temperatures, as well as high activation energy against the corrosion process. DMAEB's significant performance is primarily due to physical adsorption on the N80 C-steel surface, as confirmed by adsorption isotherms, SEM, EDX, FT-IR, and theoretical studies. Our findings shed new light on the use of Gemini surfactants as corrosion inhibitors in petroleum wells.

Today, the use of strong acids is an important source of promoting petroleum well productivity[1]. Hydrochloric acid (HCl) is injected into the N80 C-steel pipe to remove the scale layers from the pipe surface[2]. During acid washing, the strong acid causes severe corrosion in the steel pipe wall, reducing the pipe's strength and resulting in material destruction[3,4]. During the cleaning process, corrosion inhibitors are mixed with the acids as a first line of defence[5–8]. The most important source of corrosion protection for steel pipes is a group of various corrosion inhibitors such as organic compounds, inorganic compounds, and heterocyclic compounds[9–14]. Indeed, the toxic effects of these compounds compelled many researchers to use nontoxic alternatives to control corrosion in the petroleum industry.

Surfactants have recently been used to replace traditional corrosion inhibitors, providing minimal risk and mitigating environmental impacts[15–17]. In comparison to other reported corrosion inhibitors such as organic and inorganic inhibitors, the use of Gemini surfactants (GS) is the most practical additive due to many advantages such as low toxicity, no irritating odor, good thermal stability, and high efficacy.

Presently, GS is capable of corrosion inhibition in different media with very high efficacy[18,19]. GS is composed of two head groups (hydrophilic) and two tails (hydrophobic) tied with the spacer[20]. Therefore, the likely role of GS in the control of corrosion will be more effective than the conventional surfactants .Moreover; the cationic GS would provide increased anti-corrosion properties due to its antibacterial effects against the bacteria in the petroleum field.

The novelty in this work is the exploring for the first time the anti-corrosion properties of cationic Gemini surfactant, 1,2-bis(dodecyl dimethylammonio) ethane dibromide (DMAEB), for N80 C-steel pipe in the acid washing solution (15% HCl). Although many works have been conducted in the field, there is still a lack in the theoretical and mechanistic approaches. In this work, we used both experimental (chemical, electrochemical and surface inspections) and theoretical approaches to explain the mechanism of inhibition efficiency of DMAEB.

Materials and methods

Materials. An Egyptian steel company supplied N80 C-steel pipe (composition: ≈ 0.33% C, 0.24% Si, 1.45% Mn, 0.05% Nb, 0.05% V, the balance Fe). Sigma-Aldrich provided the 1,2-bis(dodecyldimethylammonio) ethane dibromide (DMAEB) (purity 98%) and HCl (purity 37%). Figure 1 depicts the molecular structure of DMAEB.

[1]Egyptian Petroleum Research Institute (EPRI), Nasr City, Cairo, Egypt. [2]Department of Chemistry, College of Sciences, Taif University, Taif, Saudi Arabia. ✉email: hamadadeiab@yahoo.com

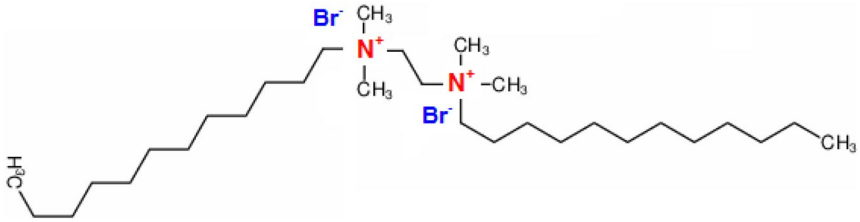

Figure 1. Molecular structure of 1,2-bis(dodecyldimethylammonio) ethane dibromide (DMAEB).

DMAEB Conc mg/l	C_R average value ± standard deviation (mg/cm²/h)	E_w%
Blank	2.84 ± 0.19	–
20	1.97 ± 0.13	30.6
40	1.02 ± 0.11	64.0
60	0.42 ± 0.05	85.2
80	0.16 ± 0.03	94.3
100	0.09 ± 0.01	96.8
120	0.10 ± 0.01	96.4
150	0.09 ± 0.01	96.8

Table 1. Corrosion parameters obtained from mass loss method for N80 C-steel pipe in 15.0% HCl solution without (blank) and with DMAEB at 303 K.

Methods. The surfaces of the N80 C-steel specimens were prepared before each experiment according to ASTM G1-03[21,22]. ASTM G31—72(2004) standard method was used to conduct the mass loss experiments and evaluating corrosion rate[23,24].

The polarization experiments were recorded using a three-electrode cell (working electrode = N80 C-steel, reference electrode = SCE, counter electrode = Pt) and potentiostat instrument (EG/G Model 273A). The polarization experiments were conducted in the potential range ± 250 mV vs. OCP and using a scan rate of 1.0 mV s^{-1}.

All measurements (potentiodynamic polarisation, gravimetry) were carried out three times under identical conditions. The averages of all data points were recorded.

The critical micelle concentration (CMC) of the DMAEB in the pure water was determined by surface tension measurements using Tensiometer (KRÜSS Scientific).

The surface morphology investigations (SEM and EDX) were conducted using ZEISS/EVO Scanning Electron Microscope fitted with EDX analyzer. FT-IR spectra were recorded via FT-IR spectrophotometer (Shimadzu: IRTracer™-100).

Quantum chemical calculations were studied using the VAMP module in Materials Studio-6.0-software from Accelrys Inc.

Results and discussion

anti-corrosion properties of DMAEB. The mass loss method and electrochemical technique (i.e. polarization test) have been used to investigate the anti-corrosion capabilities of DMAEB for N80 C-steel pipe in the acid washing solution (15% HCl).

Table 1 shows the corrosion rate (C_R) from mass loss measurements, as well as the inhibition efficiency (E_w%), for N80 C-steel pipe in 15% HCl solution with increasing concentrations of DMAEB at 303 K.

The following relationships were used to calculate the C_R and E_w%[25,26]:

$$C_R = M/t \times A, \tag{1}$$

$$E_W\% = \frac{C_{R0} - C_R}{C_{R0}} \times 100 \tag{2}$$

M is the mass loss in N80 C-steel specimen, t is the time of immersion, A is the surface area, C_{R0} is the corrosion rate for blank solution and C_R is the corrosion rate for inhibited solution.

According to Table 1, the acid solution treatment with DMAEB resulted in a decrease in C_R values. The change in DMAEB concentrations had a significant impact on the C_R values. This means that increasing DMAEB concentrations causes a decrease in C_R values.

The addition of 100 mg/l of DMAEB results in the highest inhibition efficiency (E_w% = 96.8) (Table 1). There was no significant change in the E_w% value above 100 mg/l.

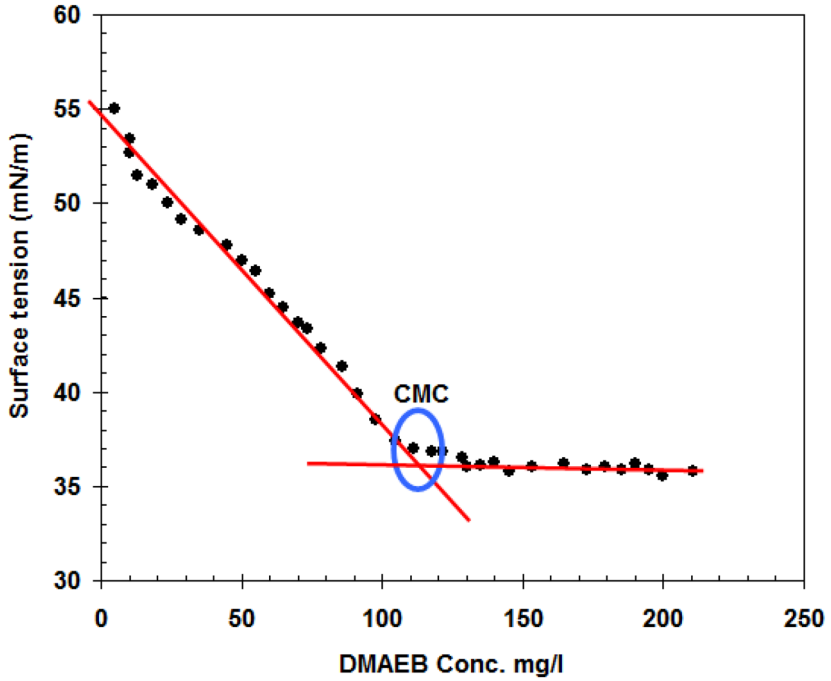

Figure 2. Variation of the surface tension with concentrations of DMAEB at 303 K.

Because the CMC of Gemini surfactant is important in determining a surfactant's inhibition efficiency[27], the CMC value of DMAEB was determined by surface tension measurements, as shown in Fig. 2. According to Fig. 2, the CMC value of DMAEB is 111 mg/l. This indicates that DMAEB's maximum performance was achieved near its CMC value. At the C-steel/solution interface, a complete monolayer of DMAEB was formed at CMC value. There are no spaces available for the adsorption of additional surfactant molecules in this case. This refers to the direct relationship between the surfactant's CMC value and corrosion inhibition.

These findings show that the cationic Gemini surfactant DMAEB has a high efficacy (96.8%) in inhibiting corrosion of N80 C-steel pipe in 15.0% HCl solution at a low concentration (100 mg/l).

The electrochemical parameters of N80 C-steel pipe were evaluated using the polarization method in both 15.0% HCl solution and blank solution treated with Gemini surfactant DMAEB. As shown in Fig. 3, the treatment of 15.0% HCl solution with DMAEB resulted in a reduction of both anodic and cathodic lines. The change in the polarization curves was found to be dependent on DMAEB concentration.

When DMAEB was added to a 15.0% HCl solution, the corrosion potential ($E_{corr.}$) shifted to the positive direction (Table 2). At 150 mg/l, the maximum shifting in $E_{corr.}$ was less than 85 mV. DMAEB was identified as the mixed-type corrosion inhibitor based on these findings[28,29]. Furthermore, the addition of DMAEB resulted in a significant decrease in corrosion current density (i_{corr}) (Table 2). While i_{corr} decreases, the changes in both Tafel line slopes (b_a for anode and b_c for cathode) remain nearly constant (Table 2). This discovery supports DMAEB's inhibitory mechanism, which involves blocking the anodic and cathodic sites by surfactant molecules[30,31].

The following relationship can be used to calculate the inhibition efficiency E_p% values based on polarization measurements[32,33]:

$$E_P\% = \frac{i_{corr(0)} - i_{corr}}{i_{corr(0)}} \times 100. \quad (3)$$

$i_{corr(0)}$ is the corrosion current density for blank solution).

The increase in DMAEB concentration is directly proportional to E_p% values. The highest DMAEB concentration, 100 mg/l, resulted in a 97% reduction in corrosion rate (Table 2).

Figure 4 depicts a histogram comparing the inhibition percentages of the two techniques (polarization and mass loss) for the same conditions. It appears that no significant differences in inhibition percentage values are observed regardless of the techniques used. The inhibition percentages obtained by mass loss measurements were found to be slightly lower than those obtained by polarization measurements. This is because the surface of N80 C-steel is exposed to the acidic solution for a longer period of time when using the mass loss method[34].

The main mechanism of the Gemini surfactant's anti-corrosion properties is based on its adsorption capability on the surface of the N80 C-steel pipe[35,36]. Because the surface of the steel in acidic solution has a positive charge, the adsorption of Cl^- ions from the solution on the steel surface is facilitated[37]. The steel surface was changed to a negatively charged surface in this case. This situation promotes electrostatic interactions between positively charged DMAEB molecules and the steel surface, resulting in the formation of the DMAEB surface layer. This surface layer protects the N80 C-steel pipe's surface from the corrosive acid solution, resulting in a low corrosion rate[38]. The short spacer group connects the two head groups in GS. This facilitates the hydrophobic interaction

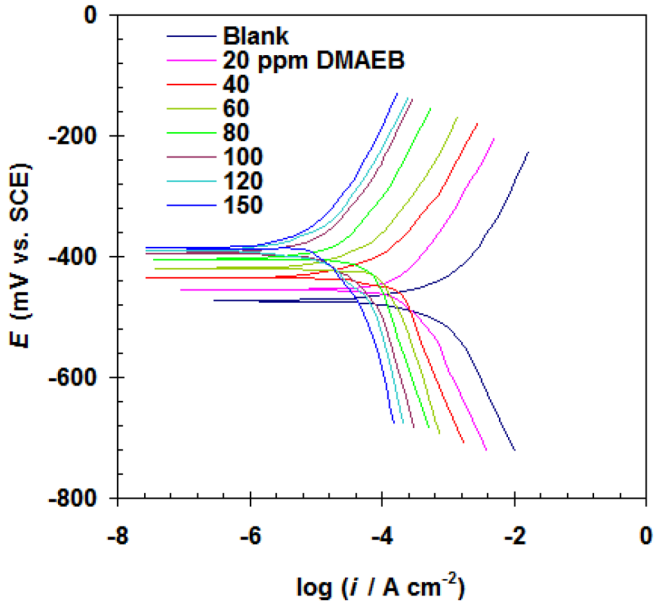

Figure 3. Polarization curves of N80 C-steel pipe in 15.0% HCl solution without (blank) and with DMAEB at 303 K.

DMAEB Conc	E_{corr}	b_a	b_c	i_{corr}	
mg/l	mV (SCE)	(mV/dec)	(mV/dec)	μA/cm^2	E_p%
Blank	− 474	75	123	623	–
20	− 455	82	120	401	35.6
40	− 435	87	112	182	70.7
60	− 419	79	133	63	89.8
80	− 404	89	143	20	96.8
100	− 398	85	127	17	97.2
120	− 394	92	128	16	97.4
150	− 390	96	126	15	96.5

Table 2. Electrochemical parameters obtained from polarization curves of N80 C-steel pipe in 15.0% HCl solution without (blank) and with DMAEB at 303 K.

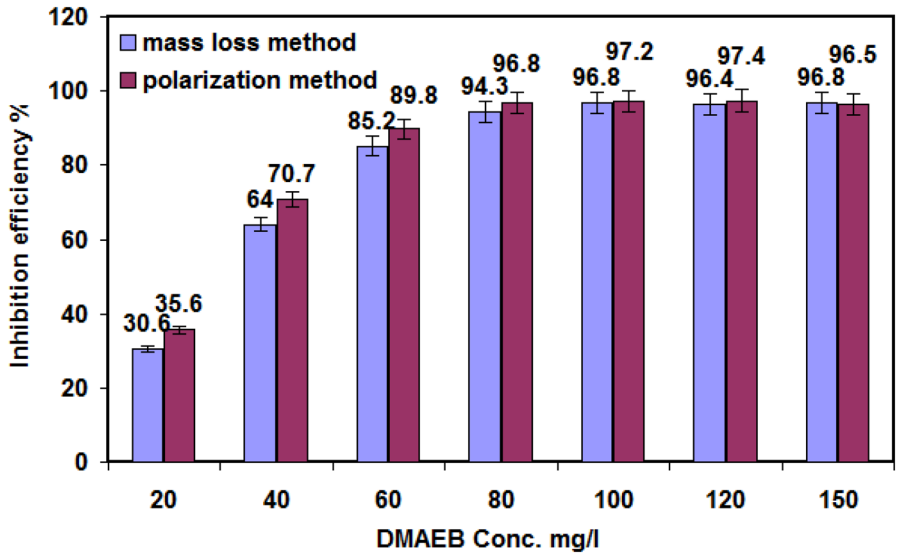

Figure 4. Comparison of inhibition efficiency% values obtained from mass loss and polarization methods.

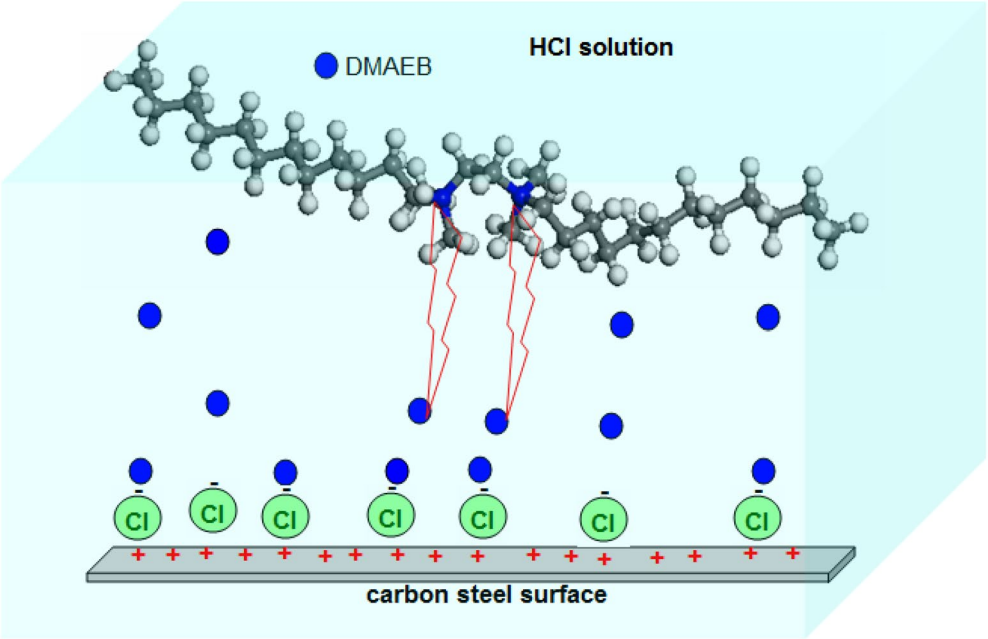

Figure 5. Schematic illustration of inhibition mechanism of DMAEB for N80 C-steel corrosion in 15.0% HCl solution.

Compounds	Conc M	Temperature K	Solution	Efficiency %	References
1,4-bis (1-Chlorobenzyl-benzimidazolyl)-butane	3.7×10^{-4}	303	0.5 M HCl	89.7	[41]
2,2′-Bipyridyl-5,5′-dimethylene-bis(*N*,*N*′-dimethylalkylammonium bromide)	1×10^{-4}	303	1 M HCl	83.4, 88.1, 88.6	[42]
n = 8, 10, and 12					
Propanediyl-1,3-bis(*N*,*N*-dihydroxyethyl-*N*-dodecylammonium bromide)	3.0×10^{-5}	298	1 M HCl	88.5	[43]
Pyridyl gemini surfactants	$\approx 1\times10^{-3}$	303	1 M HCl	90.33	[44]
bis-Quaternary ammonium salt gemini surfactan	$3.28\times10^{-}$	298	1 M HCl	90	[45]
DMAEB	1.62×10^{-4}	303	15% HCl	≈ 97	This work

Table 3. Comparison of the inhibition efficiency of DMAEB with other inhibitors of the same family for carbon steel in HCl solution reported in the literature.

between the DMAEB's two alkyl tails, lowering the CMC value. Furthermore, the short spacer group promotes the formation of more rigid molecules. This prevents DMAEB molecules from desorbing from the metal surface, resulting in increased inhibition efficiency[39]. Additionally, the long two alkyl chains help to cover the surface of the N80 C-steel pipe[40]. The schematic illustration of the inhibition mechanism is shown in Fig. 5.

DMAEB has a higher efficiency in a more corrosive solution when compared to previous works for other corrosion inhibitors of the same family in the literature[41–45] (see Table 3).

Temperature dependence and activation energy. The C_R values of the N80 C-steel pipe in 15.0% HCl solution containing 100 mg/l of DMAEB were recorded at temperatures ranging from 303 to 333 K to predict the stability of Gemini surfactant DMAEB at high temperatures (Table 4). The highest temperature (333 K), as shown in Table 4, reduced the E_w% of DMAEB to 92.5%. This finding confirms DMAEB's high stability at high temperatures. Two factors contribute to the slight decrease in E_w% of DMAEB at high temperatures. The first factor is an increase in the corrosion rate of steel as temperature rises[46]. The second factor is the high-temperature desorption of some DMAEB molecules from the steel surface (i.e. physical adsorption)[47].

The relationship between corrosion rate C_R and activation energy (E_a) is expressed by the Arrhenius formula (see Eq. 4) [48].

$$C_R = A\exp\left(\frac{-E_a}{RT}\right). \tag{4}$$

Temperature (K)	Solution	C_R (mg/cm²/h)	E_w%
303	15% HCl	2.84 ± 0.19	–
	15% HCl + 100 mg/l DMAEB	0.09 ± 0.01	96.8
313	15% HCl	2.95 ± 0.19	–
	15% HCl + 100 mg/l DMAEB	0.12 ± 0.01	95.9
323	15% HCl	3.23 ± 0.19	–
	15% HCl + 100 mg/l DMAEB	0.17 ± 0.02	94.7
333	15% HCl	4.68 ± 0.19	–
	15% HCl + 100 mg/l DMAEB	0.35 ± 0.03	92.5

Table 4. Corrosion parameters obtained from mass loss method for N80 C-steel pipe in 15% HCl solution without and with 100 mg/l DMAEB at different temperatures.

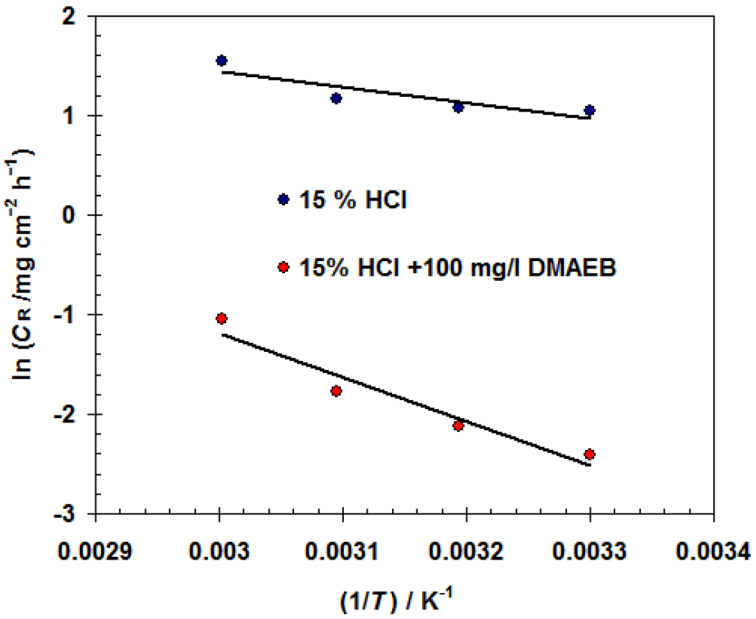

Figure 6. Arrhenius plot for N80 C-steel pipe in 15.0% HCl solution without and with 100 mg/l DMAEB.

The E_a was calculated using the Arrhenius plot (straight-line gradient) (see Fig. 6).

The calculated E_a for the corrosion reaction in 15.0% HCl solution containing 100 mg/l of DMAEB is 36.74 kJ/mol, which is comparable to the calculated E_a in 15.0% HCl solution (13.08 kJ/mol). This finding confirms that the presence of DMAEB in a 15.0% HCl solution raises the energy barrier for corrosion, resulting in a low corrosion rate[49–51].

Adsorption isotherm studies. Because the effectiveness of Gemini surfactant DMAEB is dependent on DMAEB molecules' adsorption capability on the steel surface, it is critical to investigate the adsorption isotherm in this section. The Langmuir adsorption isotherm (Eq. 5) is the best fitting isotherm that describes the adsorption process of DMAEB molecules based on mass loss measurements[52].

$$\frac{C_{\text{inh}}}{\theta} = \frac{1}{K_{\text{ads}}} + C_{\text{inh}}. \tag{5}$$

θ is the surface coverage = E_w%/100, C_{inh} is the DMAEB concentration, K_{ads} is the equilibrium constant).

The linear correlation coefficient (R^2) is very close to one in the Langmuir isotherm plot (Fig. 7), confirming the validity of this isotherm[53]. The DMAEB's K_{ads} was determined to be 1.72×10^4 M^{-1}.

Gibbs free energy change ($\Delta G°_{ads}$) was calculated from the following relation[54]:

$$\Delta G^{\circ}_{\text{ads}} = -RT\ln(55.5K_{\text{ads}}). \tag{6}$$

The $\Delta G°_{ads}$ for the DMAEB was identified to be − 34.62 kJ/mol. A negative $\Delta G°_{ads}$ value confirms the spontaneity of DMAEB adsorption on the steel surface[55]. The value of $\Delta G°_{ads}$ (i.e. − 34.62 kJ/mol) refers to DMAEB physisorption on the surface of the N80 C-steel[56].

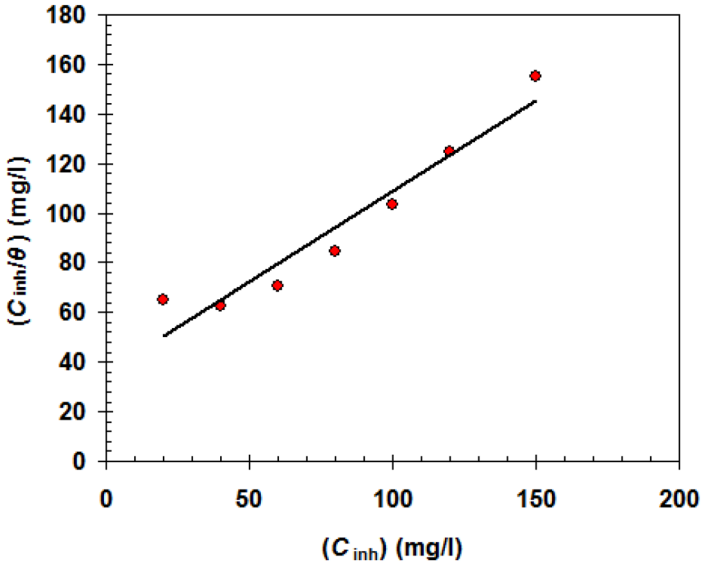

Figure 7. Langmuir isotherm plot for N80 C-steel pipe in 15.0% HCl solution containing 100 mg/l DMAEB at 303 K.

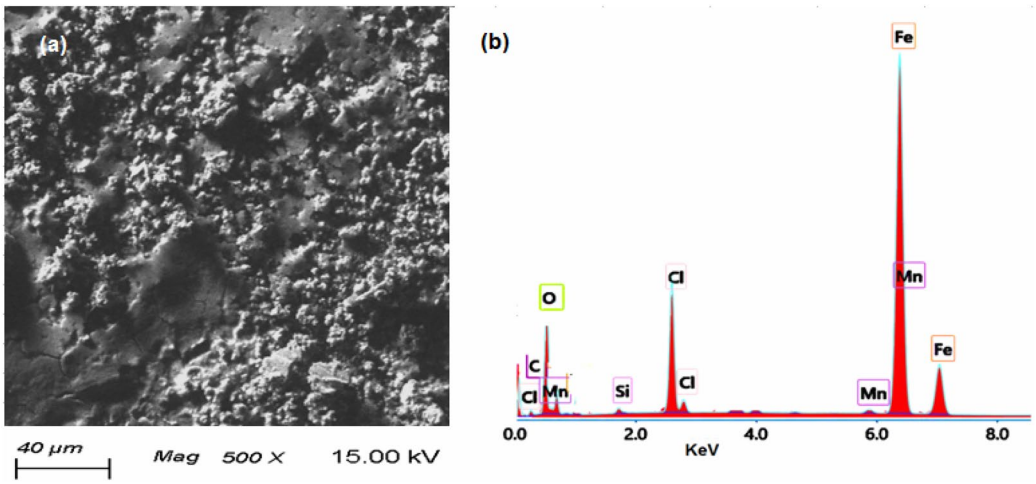

Figure 8. (**a**) SEM image and (**b**) EDX spectra for N80 C-steel pipe after immersion in the blank solution (15.0% HCl).

Surface analysis. The morphological analysis (SEM and EDX) of the N80 C-steel in the blank solution (15.0% HCl) and inhibited solution (15.0% + 100 mg/l DMAEB) are presented in Figs. 8 and 9. In the blank solution, the surface morphology of the N80 C-steel revealed a damaged structure and dense surface roughness (Fig. 8a). The N80 C-steel EDX spectrum in the blank solution (Fig. 8b) revealed characterized signals for N80 C-steel composition and corrosion products (i.e. O, Cl, C, Mn, Si, and Fe).

In the presence of 100 mg/l DMAEB, the N80 C-steel has a smooth surface and is free of corrosion products (Fig. 9a). The presence of characterized DMAEB signals is revealed by the EDX spectrum of N80 C-steel in inhibited solution (Fig. 9b) (i.e. N and C). Furthermore, Cl signals have vanished.

The FT-IR spectra of pure DMAEB and the film formed on the surface of N80 C-steel in the inhibited solution (15.0% HCl + 100 mg/l DMAEB) were analyzed and shown in Fig. 10. The characteristic peaks for C–H stretch, CH_2 bending, CH_3 bending, C–C stretch, C–N, and long-chain CH_2 groups can be seen in the FT-IR spectrum of pure DMAEB.

The FT-IR spectra of the film formed on the surface of N80 C-steel in the inhibited solution showed three changes. The first is a shift in some peaks, such as C–H stretch, CH_2 bending, CH_3 bending, and C–C stretch. The second change is the absence of C–N. The presence of new peaks related to Fe–N bonds at 645–450 cm^{-1} is the third change. All of these studies support the adsorption of DMAEB molecules on N80 C-steel.

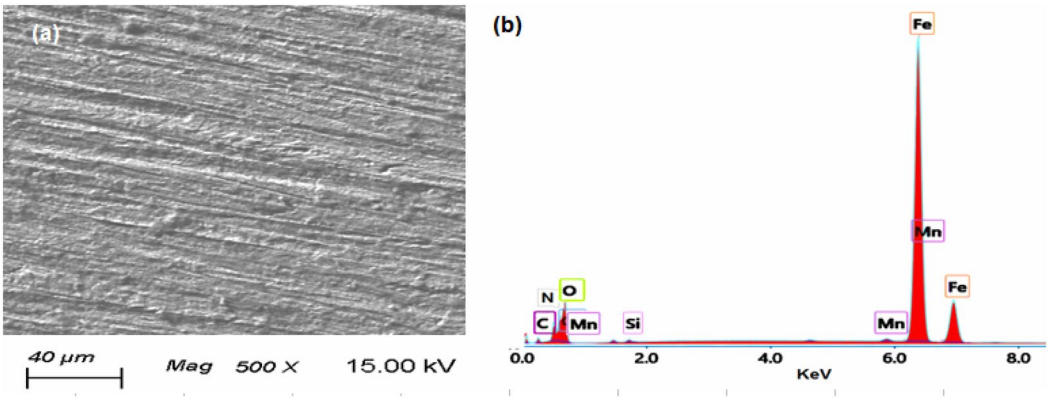

Figure 9. (**a**) SEM image and (**b**) EDX spectra for N80 C-steel pipe after immersion in the inhibited solution (15.0% HCl + 100 mg/l DMAEB).

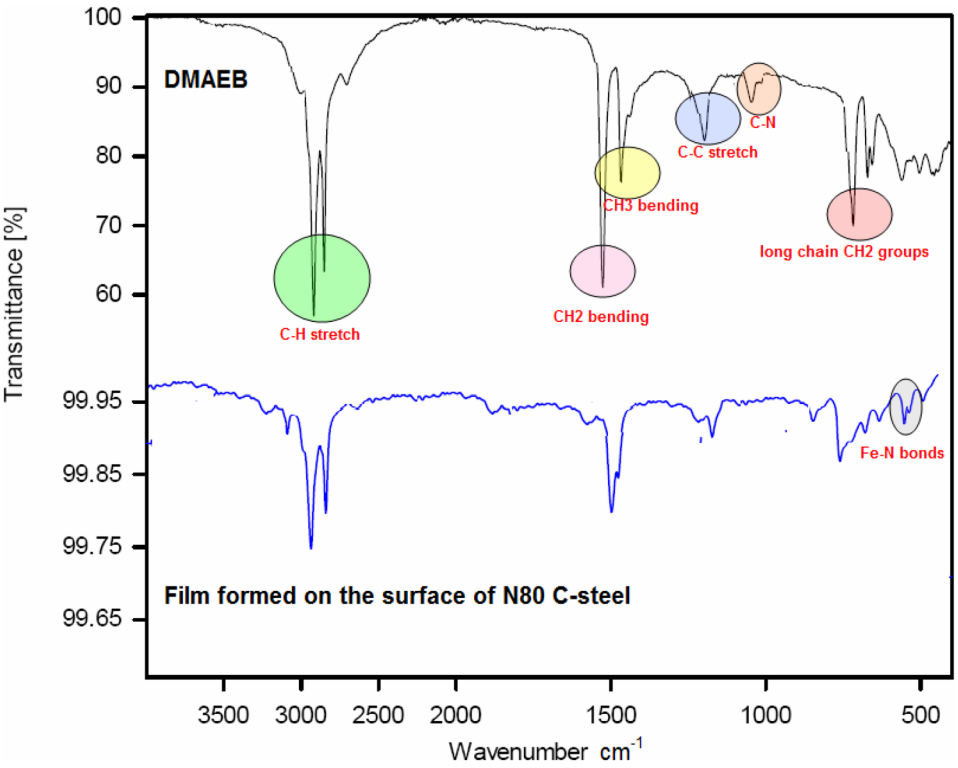

Figure 10. FT-IR spectra of pure DMAEB and film formed on the surface of N80 C-steel in the inhibited solution (15.0% HCl + 100 mg/l DMAEB).

Quantum chemical calculations. Quantum chemical calculations were used to support the experimental results. Figure 11a,b show that HOMO (highest occupied molecular orbital) and LUMO (lowest unoccupied molecular orbital) regions are concentrated on ammonium groups. This demonstrates that the ammonium groups in DMAEB molecules are the active components in the adsorption process[31]. The high value of the HOMO energy (E_{HOMO} = 8.939 eV) refers to the DMAEB molecule's ability to link with the steel surface[57]. Also, the low LUMO energy (E_{LUMO} = 1.577 eV) refers to the DMAEB molecule's ability to gain electrons from the filled Fe d-orbital[58]. Furthermore, the low energy gap ($\Delta E = E_{LUMO} - E_{HOMO}$, 7.362 eV) refers to DMAEB molecules' high inhibition performance[59]. It was discovered that the electron density was distributed throughout the entire DMAEB molecule (see Fig. 11c). This means that DMAEB molecules are adsorbing on the Fe surface in flat-lying orientations[60].

DMAEB's high dipole moment (i.e. µ = 6.94 Debye) indicates a strong electrostatic interaction between DMAEB molecules and the C-steel surface[61].

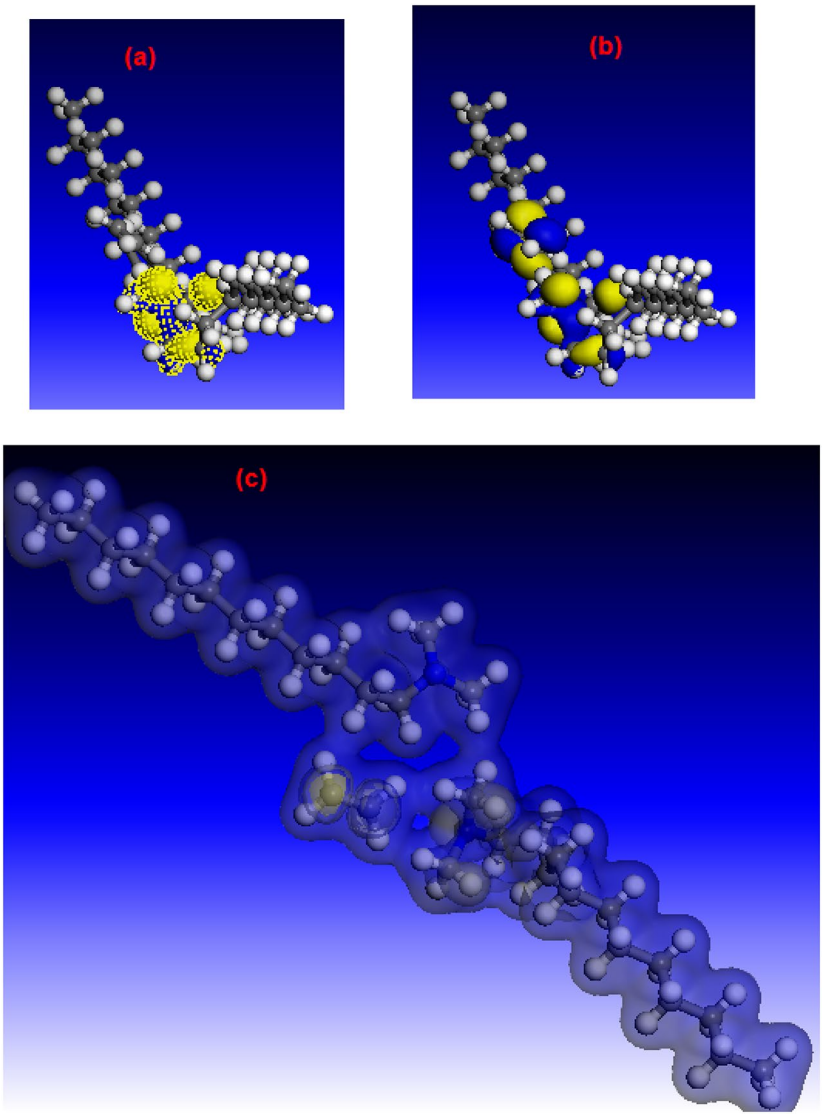

Figure 11. (**a**) HOMO, (**b**) LUMO and (**c**) total electron density distribution for DMAEB molecule. "Computational results obtained using software programs from Accelrys Software Inc. The ab initio calculations were performed with the DMol^3 program, and graphical displays generated with Materials Studio".

The electronegativity (χ) and global hardness (η) parameters for DMAEB are calculated from the following relations:

$$\chi = 0.5 \times (I + A), \tag{7}$$

$$\eta = 0.5 \times (I - A), \tag{8}$$

where I is the ionization potential = $-E_{HOMO}$ and A is the electron affinity = $-E_{LUMO}$.

The calculated values of χ and η are 5.258 eV and 3.681 eV, respectively.

The high χ value for DMAEB molecules indicates a high ability to attract electrons and, as a result, a high adsorption efficiency[62]. Furthermore, the low η value for DMAEB molecules indicates a strong interaction between the metal surface and inhibitor molecules[63].

Conclusions

In summary, we investigated the anti-corrosion properties of cationic Gemini surfactant, 1,2-bis(dodecyldimethylammonio) ethane dibromide (DMAEB), for N80 C-steel pipe in the acid washing solution (15% HCl).

It is worth noting that the Gemini surfactant DMAEB has a high efficacy (96.8%) in inhibiting corrosion of N80 C-steel pipe in 15.0% HCl solution at a low concentration (100 mg/l). DMAEB's anti-corrosion properties were investigated using mass loss, polarization, SEM, EDX, and FT-IR tools. DMAEB acts as a mixed-type

corrosion inhibitor, as evidenced by the polarization curves. The high temperature (333 K) slightly reduced DMAEB efficacy to 92.5%, confirming DMAEB's high stability at high temperatures. Furthermore, the presence of DMAEB in a 15.0% HCl solution raises the energy barrier for corrosion, resulting in a low corrosion rate. The Langmuir adsorption isotherm accurately described the adsorption of DMAEB molecules. The ΔG°_{ads} was − 34.62 kJ/mol, indicating physisorption behavior. SEM, EDX, and FT-IR analysis confirmed the adsorption of DMAEB molecules on the surface of N80 C-steel. To back up the experimental findings, quantum chemical calculations were used.

Received: 26 January 2021; Accepted: 6 May 2021
Published online: 18 May 2021

References

1. Jiawei, K., Yan, J., Kunpeng, Z. & Pengju, R. Experimental investigation on the characteristics of acid-etched fractures in acid fracturing by an improved true tri-axial equipment. *J. Pet. Sci. Eng.* **184**, 106471 (2020).
2. Yadav, M., Sarkar, T. K. & Purkait, T. Amino acid compounds as eco-friendly corrosion inhibitor for N80 steel in HCl solution: Electrochemical and theoretical approaches. *J. Mol. Liq.* **212**, 731–738 (2015).
3. Brylee, D. B. & Rigoberto, C. A. Polymeric corrosion inhibitors for the oil and gas industry: Design principles and mechanism. *React. Funct. Polym.* **95**, 25–45 (2015).
4. Zheng, X., Zhang, S., Li, W., Gong, M. & Yin, L. Experimental and theoretical studies of two imidazolium-based ionic liquids as inhibitors for mild steel in sulfuric acid solution. *Corros. Sci.* **95**, 168–179 (2015).
5. Zhang, Q. H. *et al.* Two novel chitosan derivatives as high efficient eco-friendly inhibitors for the corrosion of mild steel in acidic solution. *Corros. Sci.* **164**, 108346 (2020).
6. Sarkar, T. K., Saraswat, V., Mitra, R. K., Obot, I. B. & Yadav, M. Mitigation of corrosion in petroleum oil well/tubing steel using pyrimidines as efficient corrosion inhibitor: Experimental and theoretical investigation. *Mater. Today Commun.* **26**, 101862 (2021).
7. Tiwari, N., Mitra, R. K. & Yadav, M. Corrosion protection of petroleum oil well/tubing steel using thiadiazolines as efficient corrosion inhibitor: Experimental and theoretical investigation. *Surf. Interfaces* **22**, 100770 (2021).
8. Saraswat, V. & Yadav, M. Carbon dots as green corrosion inhibitor for mild steel in HCl solution. *ChemistrySelect* **5**, 7347–7357 (2020).
9. Yadav, M., Sarkar, T. K. & Purkait, T. Studies on adsorption and corrosion inhibitive properties of indoline compounds on N80 steel in hydrochloric acid. *J. Mater. Eng. Perform.* **24**, 4975–4984 (2015).
10. Yadav, M., Behera, D., Kumar, S. & Yadav, P. Experimental and quantum chemical studies on corrosion inhibition performance of thiazolidinedione derivatives for mild steel in hydrochloric acid solution. *Chem. Eng. Commun.* **202**, 303–315 (2015).
11. Yadav, M., Kumar, S., Kumari, N., Bahadur, I. & Ebenso, E. E. Experimental and theoretical studies on corrosion inhibition effect of synthesized benzothiazole derivatives on mild steel in 15% HCl solution. *Int. J. Electrochem. Sci.* **10**, 602–624 (2015).
12. Singh, A. *et al.* Comprehensive investigation of steel corrosion inhibition at macro/micro level by ecofriendly green corrosion inhibitor in 15% HCl medium. *J. Colloid Interface Sci.* **560**, 225–236 (2020).
13. Fayomi, O. S. I., Popoola, A. P. I. & Joseph, O. O. Assessment of potassium chromate inhibition and adsorption on type A513 mild steel in simulated contaminated media. *Energy Proc.* **119**, 883–890 (2017).
14. Obot, I. B., Umoren, S. A., Gasem, Z. M., Suleiman, R. & El Ali, B. Theoretical prediction and electrochemical evaluation of vinylimidazole and allylimidazole as corrosion inhibitors for mild steel in 1M HCl. *J. Ind. Eng. Chem.* **21**, 1328–1339 (2015).
15. Deyab, M. A. M. Corrosion inhibition and adsorption behavior of sodium lauryl ether sulfate on L80 carbon steel in acetic acid solution and its synergism with ethanol. *J. Surfactants Deterg.* **18**, 405–411 (2015).
16. Deyab, M. A. Hydrogen generation during the corrosion of carbon steel in crotonic acid and using some organic surfactants to control hydrogen evolution. *Int. J. Hydrog. Energy* **38**, 13511–13519 (2013).
17. Wang, D., Li, Y., Chen, B. & Zhang, L. Novel surfactants as green corrosion inhibitors for mild steel in 15% HCl: Experimental and theoretical studies. *Chem. Eng. J.* **402**, 126219 (2020).
18. Pakiet, M. *et al.* Gemini surfactant as multifunctional corrosion and biocorrosion inhibitors for mild steel. *Bioelectrochemistry* **128**, 252–262 (2019).
19. Zhou, T., Yuan, J., Zhang, Z., Xin, X. & Guiying, Xu. The comparison of imidazolium Gemini surfactant $[C_{14}\text{-}4\text{-}C_{14}im]Br_2$ and its corresponding monomer as corrosion inhibitors for A3 carbon steel in hydrochloric acid solutions: Experimental and quantum chemical studies. *Colloids Surf. A* **575**, 57–65 (2019).
20. Shen, T. & Gao, M. Gemini surfactant modified organo-clays for removal of organic pollutants from water: A review. *Chem. Eng. J.* **375**, 121910 (2019).
21. ASTM G1-03(2017)e1. *Standard Practice for Preparing, Cleaning, and Evaluating Corrosion Test Specimens* (ASTM International, 2017) www.astm.org.
22. Deyab, M. A., De Riccardis, A. & Mele, G. Novel epoxy/metal phthalocyanines nanocomposite coatings for corrosion protection of carbon steel. *J. Mol. Liq.* **220**, 513–517 (2016).
23. ASTM G31-72. *Standard Practice for Laboratory Immersion Corrosion Testing of Metals* (ASTM International, 2004) www.astm.org.
24. Deyab, M. A. The inhibition activity of butylated hydroxyl toluene towards corrosion of carbon steel in biodiesel blend B20. *J. Taiwan Inst. Chem. Eng.* **60**, 369–375 (2016).
25. Aslam, R. *et al.* Sugar based N, N′-didodecyl-N, N′digluconamideethylenediamine gemini surfactant as corrosion inhibitor for mild steel in 3.5% NaCl solution-effect of synergistic KI additive. *Sci. Rep.* **8**, 3690 (2018).
26. Deyab, M. A. Corrosion inhibition of heat exchanger tubing material (titanium) in MSF desalination plants in acid cleaning solution using aromatic nitro compounds. *Desalination* **439**, 73–79 (2018).
27. Chaudhary, N. K., Bhattarai, A., Guragain, B. & Bhattarai, A. Conductivity, surface tension, and comparative antibacterial efficacy study of different brands of soaps of Nepal. *J. Chem.* **2020**, 6989312 (2020).
28. Mashuga, M. E. *et al.* Adsorption, thermodynamic and quantum chemical studies of 1-hexyl-3-methylimidazolium based ionic liquids as corrosion inhibitors for mild steel in HCl. *Materials* **8**, 3607–3632 (2015).
29. Deyab, M. A. *et al.* $NaNi(H_2PO_3)_3{\cdot}H_2O$ as a novel corrosion inhibitor for X70-steel in saline produced water. *J. Mol. Liq.* **216**, 636–640 (2016).
30. Gerengi, H., Mielniczek, M., Gece, G. & Solomon, M. M. Experimental and quantum chemical evaluation of 8-Hydroxyquinoline as a corrosion inhibitor for copper in 0.1 M HCl. *Ind. Eng. Chem. Res.* **55**, 9614–9624 (2016).
31. Deyab, M. A., Osman, M. M., Elkholy, A. E. & El-Taib Heakal, F. Green approach towards corrosion inhibition of carbon steel in produced oilfield water using lemongrass extract. *RSC Adv.* **7**, 45241–45251 (2017).
32. Abd El-Rehim, S. S., Hassan, H. H., Deyab, M. A. & El Moneim, A. A. Experimental and theoretical investigations of adsorption and inhibitive properties of Tween 80 on corrosion of aluminum alloy (A5754) in alkaline media. *Z. Phys. Chem.* **230**, 67–78 (2016).

33. Cao, S. *et al.* Green Brönsted acid ionic liquids as novel corrosion inhibitors for carbon steel in acidic medium. *Sci. Rep.* **7**, 8773 (2017).
34. Khamaj, J. A. Comparison of potentiodynamic polarization and weight loss measurement techniques in the study of corrosion behavior of 6061 Al/SiC composite in 3.5 M NaCl solution, Asian. *J. Appl. Sci.* **3**, 264–270 (2015).
35. Kaczerewsk, O., Leiva-GarciabR, R., Aki, B., Brycki, I. & Kowalczyk, T. P. Effectiveness of O-bridged cationic gemini surfactants as corrosion inhibitors for stainless steel in 3 M HCl: Experimental and theoretical studies. *J. Mol. Liq.* **249**, 1113–1124 (2018).
36. Deyab, M. A., Rachid Ouarsal, A. M., Al-Sabagh, M. L. & El Bali, B. Enhancement of corrosion protection performance of epoxy coating by introducing new hydrogenphosphate compound. *Prog. Org. Coat.* **107**, 37–42 (2017).
37. Ma, Y., Han, F., Li, Z. & Xia, C. Acidic-functionalized ionic liquid as corrosion inhibitor for 304 stainless steel in aqueous sulfuric acid. *ACS Sustain. Chem. Eng.* **4**, 5046–5052 (2016).
38. Deyab, M. A. Electrochemical investigations on pitting corrosion inhibition of mild steel by provitamin B5 in circulating cooling water. *Electrochim. Acta* **202**, 262–268 (2016).
39. Yao, S.-Z., Jiang, X.-H., Zhou, L.-M., Lv, Y.-J. & Hu, X.-Q. Corrosion inhibition of iron in 20% hydrochloric acid by 1,4/1,6-bis(α-octylpyridinium)butane/hexane dibromide. *Mater. Chem. Phys.* **104**, 301–305 (2007).
40. Deyab, M. A. Efficiency of cationic surfactant as microbial corrosion inhibitor for carbon steel in oilfield saline water. *J. Mol. Liq.* **255**, 550–555 (2018).
41. Wang, X., Yang, H. & Wang, F. A cationic gemini-surfactant as effective inhibitor for mild steel in HCl solutions. *Corros. Sci.* **52**, 1268–1276 (2010).
42. Feng, L. *et al.* Cationic Gemini surfactants with a bipyridyl spacer as corrosion inhibitors for carbon steel. *ACS Omega* **3**, 18990–18999 (2018).
43. Yin, C. *et al.* Influence of hydroxyl groups on the inhibitive corrosion of Gemini surfactant for carbon steel. *ACS Omega* **5**, 2620–2629 (2020).
44. Han, T., Guo, J., Zhao, Q., Wu, Y. & Zhang, Y. Enhanced corrosion inhibition of carbon steel by pyridyl gemini surfactants with different alkyl chains. *Mater. Chem. Phys.* **240**, 122156 (2020).
45. Zhang, J. *et al.* A dissymmetric bis-quaternary ammonium salt gemini surfactant as effective inhibitor for Q235 steel in hydrochloric acid. *Prog. Org. Coat.* **75**, 284–291 (2012).
46. Singh, P., Ebenso, E. E., Olasunkanmi, L. O., Obot, I. B. & Quraishi, M. A. Electrochemical, theoretical and surface morphological studies of corrosion inhibition effect of green naphthyridine derivatives on mild steel in hydrochloric acid. *J. Phys. Chem. C.* **120**, 3408–3419 (2016).
47. Verma, C., Quraishi, M., Olasunkanmi, L. O. & Ebenso, E. E. L-Proline-promoted synthesis of 2-amino-4-arylquinoline-3-carbonitriles as sustainable corrosion inhibitors for mild steel in 1 M HCl: Experimental and computational studies. *RSC Adv.* **5**, 85417–85430 (2015).
48. Wells, T. & Melchers, R. E. Modelling concrete deterioration in sewers using theory and field observations. *Cem. Concr. Res.* **77**, 82–96 (2015).
49. Loto, R. T. Surface coverage and corrosion inhibition effect of Rosmarinus officinalis and zinc oxide on the electrochemical performance of low carbon steel in dilute acid solutions. *Results Phys.* **8**, 172–179 (2018).
50. Gowraraju, N. D. *et al.* Adsorption characteristics of Iota-carrageenan and Inulin biopolymers as potential corrosion inhibitors at mild steel/sulphuric acid interface. *J. Mol. Liq.* **232**, 9–19 (2017).
51. Yadav, M., Behera, D., Kumar, S. & Sinha, R. R. Experimental and quantum chemical studies on the corrosion inhibition performance of benzimidazole derivatives for mild steel in HCl. *Ind. Eng. Chem. Res.* **52**, 6318–6328 (2013).
52. Bhuvaneshwari, B., Selvaraj, A., Iyer, N. R. & Ravikumar, L. Electrochemical investigations on the performance of newly synthesized azomethine polyester on rebar corrosion. *Mater. Corros.* **66**, 387–395 (2015).
53. Verma Chandrabhan, Q. M. A., Kluza, K., Makowska-Janusik, M., Olasunkanmi, L. O. & Ebenso, E. E. Corrosion inhibition of mild steel in 1M HCl by D-glucose derivatives of dihydropyrido [2,3-d:6,5-d′] dipyrimidine-2, 4, 6, 8(1H,3H, 5H,7H)-tetraone. *Sci. Rep.* **7**, 44432 (2017).
54. Kaskah, S. E. *et al.* Surface protection of low carbon steel with *N*-acyl sarcosine derivatives as green corrosion inhibitors. *Surf. Interfaces* **9**, 70–78 (2017).
55. Loto, R. T. & Wei, X. Electrochemical analysis of the corrosion inhibition properties of 4-hydroxy-3-methoxybenzaldehyde on low carbon steel in dilute acid media. *Cogent Eng.* **3**, 1. https://doi.org/10.1080/23311916.2016.1242107 (2016).
56. Radwan, A. B. *et al.* Enhancing the corrosion resistance of reinforcing steel under aggressive operational conditions using behentrimonium chloride. *Sci. Rep.* **9**, 18115 (2019).
57. Murulana, L. C., Singh, A. K., Shukla, S. K., Kabanda, M. M. & Ebenso, E. E. Experimental and quantum chemical studies of some Bis(trifluoromethyl-sulfonyl) imide imidazolium-based ionic liquids as corrosion inhibitors for mild steel in hydrochloric acid solution. *Ind. Eng. Chem. Res.* **51**, 13282–13299 (2012).
58. Bartley, J. *et al.* Computer simulation of the corrosion inhibition of copper in acidic solution by alkyl esters of 5-carboxybenzotriazole. *Corros. Sci.* **45**, 81–96 (2003).
59. Madkour, L. & Elroby, S. K. Inhibitive properties, thermodynamic, kinetics and quantum chemical calculations of polydentate Schiff base compounds as corrosion inhibitors for iron in acidic and alkaline media. *Int. J. Ind. Chem.* **6**, 165–184 (2015).
60. Deyab, M. A., Fouda, A. S. & Abdel-Fattah, S. New heterocyclic derivative to stop carbon steel corrosion. *Z. Phys. Chem.* **234**, 63–73 (2020).
61. Gece, G. The use of quantum chemical methods in corrosion inhibitor studies. *Corros. Sci.* **50**, 2981–2992 (2008).
62. Chermette, H. Chemical reactivity indexes in density functional theory. *J. Comput. Chem.* **20**, 129–154 (1999).
63. Guo, L. *et al.* Theoretical evaluation of the corrosion inhibition performance of 1,3-thiazole and its amino derivatives. *Arab. J. Chem.* **10**, 121–130 (2017).

Acknowledgements

Taif University Researchers Supporting Project number (TURSP-2020/19),Taif University, Saudi Arabia.

Author contributions

M.A.D. Conceptualization; Data curation; Formal analysis; Investigation; Methodology; Project administration; Resources; Software; Supervision; Validation; Visualization; Roles/Writing—original draft; Writing—review & editing. Q.M. Funding acquisition; Software; Writing—review & editing.

Competing interests

The authors declare no competing interests.

Additional information

Correspondence and requests for materials should be addressed to M.A.D.